DENTAL MATERIALS 35 (2019) e286–e297

Available online at www.sciencedirect.com

ScienceDirect

journal homepage: www.intl.elsevierhealth.com/journals/dema

Experimental composites of polyacrilonitrile-electrospun nanofibers containing nanocrystal cellulose

Bernardo U. Peres[a], *Adriana P. Manso*[a], *Luana D. Carvalho*[a], *Frank Ko*[b], *Tom Troczynski*[b], *Hugo A. Vidotti*[c], *Ricardo M. Carvalho*[a,*]

[a] *Department of Oral Biological and Medical Sciences, Division of Biomaterials, The University of British Columbia, Faculty of Dentistry, 368-2199 Wesbrook Mall, Vancouver, BC V6T 1Z3, Canada*

[b] *Department of Materials Engineering, The University of British Columbia, Faculty of Applied Sciences, 309-6350 Stores Road, Vancouver, BC V6T 1Z4, Canada*

[c] *Department of Prosthodontics, University of Western São Paulo, Presidente Prudente, São Paulo, Brazil*

ARTICLE INFO

Keywords:
Nanofibers
Electrospinning
Polyacrylonitrile
Nanocrystal cellulose
Resin composite
Flexural properties

ABSTRACT

Objective. To test the effects of addition of polyacrilonitrile (PAN) nanofibers and nanocrystal cellulose (NCC)-containing PAN nanofibers on flexural properties of experimental dental composites.

Methods. 11 wt% PAN in dimethylformamide (DMF) solution was electrospun at 17.2 kVA and 20 cm from the collector drum. NCC was added to the solution at 3 wt%. Fiber mats were produced in triplicates and tested as-spun. Strips (5 cm × 0.5 cm) were cut from the mat in an orientation parallel and perpendicular to the rotational direction of the collector drum. Tensile tests were performed and ultimate tensile strength (UTS), elastic modulus (E) and elongation at maximum stress (%) were calculated from stress/strain plots. Fiber mats were then infiltrated by resin monomers (50/50 BisGMA/TEGDMA wt%), stacked in a mold (2 × 15 × 25) and light-cured. Beams (2 × 2 × 25 mm) were cut from the slabs and tested in a universal testing machine. Data were analyzed by multiple t-test and one-way ANOVA ($\alpha = 0.05$).

Results. Addition of 3% NCC resulted in higher tensile properties of the fibers. Fibers presented anisotropic behavior with higher UTS and E when tested in perpendicular orientation. The incorporation of 3% NCC–PAN nanofibers resulted in significant increase in work of fracture and flexural strength of experimental dental composite beams.

Significance. NCC was found to be a suitable nanoparticle to reinforce experimental dental composites by incorporation via nanofiber. This fundamental study warrants future investigation in the use of electrospun nanofibres as a way to reinforce dental composites.

* *Corresponding author at*: 2199 Wesbrook Mall, JBM 368, Vancouver, BC V6T 1Z3, Canada.
E-mail address: rickmc@dentistry.ubc.ca (R.M. Carvalho).

https://doi.org/10.1016/j.dental.2019.08.107

1. Introduction

Di-methacrylate composites are widely and successfully used in clinical dentistry as the material of choice for most of the procedures requiring reconstruction of missing tooth structure [1]. Over longer-term, bulk fracture of the restorative material has been regarded as one of the major cause of failure that requires replacement [2,3]. To overcome the problem, reinforcement of the material to make it more durable is desirable. Among several approaches to address that issue, strengthening of dental composites with electrospun nanofibers has been recently the focus of some research. Fibers have been incorporated into resin matrices either as particles reconditioned from fibers [4,5] or as continuous fibers [6–8]. Although some disagreement exists from the reports [9,10], it appears that the general conclusions indicate that the presence of nanofibers increases the energy necessary to break dental composites.

Electrospinning technology made possible the combination of nanoparticles with nanofibers, creating the so-called multifunctional composite nanofibers [11]. Such technique can be used to increase the mechanical properties of regular polymeric nanofibers significantly [12,13]. Up to date, few studies have tried to investigate the effects of nanofibrous composites as reinforcing agents for dental composites [14,15].

Nanocrystalline cellulose (NCC) is a renewable, biocompatible, and extremely strong rod-like particle [16]. It has been shown that low concentrations of NCC can remarkably increase mechanical properties of electrospun nanofibers [17,18], and glass-ionomer cements [19].

Polyacrilontrile nanofibers are known for its high toughness and high strength at low weight ratio [20,21], and have already been demonstrated to reinforce dental composites positively [6]. However, to the best of our knowledge, there is no report combining NCC and PAN to reinforce dental composites. Expectedly, the use of a particle-reinforced nanofiber to reinforce a resin matrix would combine the effects to result in a fiber-reinforced composite with superior properties. We have previously demonstrated that the tensile properties of PAN nanofibers could be significantly improved by the addition of 1–3% NCC to the electrospun polymer [22]. In this study, we tested the hypothesis that the addition of NCC-reinforced PAN nanofibers to di-methacrylate resin blends could improve the flexural properties of the resultant composite. The null hypothesis tested was that there would be no effect on flexural properties of experimental dental composites when reinforced with PAN nanofibers and NCC-containing PAN nanofibers.

2. Materials and methods

2.1. Production of PAN nanofibers

Polyacrylonitrile (PAN) powder (Mw = 150,000 g/mol, Scientific Polymer Products, Ontario, NY, USA) was dissolved in *N*,*N*-dimethylformamide (DMF) (Fisher Scientific, Waltham, MA, USA) to produce polymer nanofibers. 2.2 g of PAN and 17.8 g of DMF were weighed in an analytical balance (Shimadzu, ATX 124, Kyoto, Japan) yielding a final concentration of 11 w/w%. The solution was stirred overnight at room temperature, and the viscosity was measured by a viscometer (Viscomate Model VM-10A, CBC Co. Ltd., Tokyo, Japan) prior electrospinning (viscosity range: 430–445 mPa s). The solution was then immediately transferred to a plastic syringe and fit to a Nanofiber Electrospinning Unit (NEU — Kato Tech, Japan). Electrospinning parameters were set as applied voltage at 17.2 kVA; distance between the needle tip and the collector plate at 20 cm; target speed at 2 m/min; and transverse speed at 1 cm/min. Syringe pump speed varied between 0.05–0.1 mm/min to keep a clear and visible Taylor cone. Temperature and humidity in the chamber were monitored. Air humidity was maintained between 30 and 50% and temperature varied between 24 and 27 °C. The collector plate was covered with aluminum foil, and the fibers were produced over 48 h. Fibers were collected in a random mode, and no attempt to align them was made. The formed fiber mat was gently removed from the collector plate and stored in a sealed plastic bag away from heat and humidity until use.

2.2. Production of NCC-containing nanofibers

The fiber group containing 3% NCC was done by the mixing NCC to the PAN polymer solution. First, 0.066 g of NCC powder was weighted in an analytical balance (Shimadzu, ATX 124, Kyoto, Japan) and mixed with 20 g of 11% PAN polymer solution by vortex mixing (Digital Vortex Mixer, Fisher Scientific, Waltham MA, USA) for 5 min at 3000 rpm. After vortex mixing, the vial was sealed and sonicated in ice-cold water bath (Whaledent Biosonic U100, Coltene, Ohio, USA) for 2 h. Every 15 min, the bath was filled with small amounts of ice to avoid overheating the mixture during sonication. The suspension was then placed to rest at room temperature for 15 min and the viscosity was measured. The suspension was then transferred to the electrospinning unit and nanofibers were produced with the parameters described above.

2.3. Viscosity measurements

All viscosity measurements were done using a viscometer (Viscomate Model VM-10A, CBC Co. Ltd., Tokyo, Japan) at room temperature and immediately prior electrospinning. There were three batches of PAN 11% with and without 3% NCC. The mean viscosity values were measured three times for each batch of polymeric solution (PAN 11% with and without the addition of 3% NCC).

2.4. Nanofiber mats properties

2.4.1. Tensile properties of nanofibers mats

The tensile properties of the nanofiber mats were determined by testing machine (KES-G1 Kawabata, Kato Tech Co, Kyoto, Japan) with an elongation rate of 0.2 mm/s. As-spun mats were tested in two orientations: parallel (PAR) and perpendicular (PER) to the rotational direction of the collector drum. Strips (5 cm × 0.5 cm) were cut from the mat following the orientations above and mounted in a custom jig that yields a gauge length of 4 mm.

The nanofiber mats were produced in triplicates. The central area (5 cm away from the edges of the aluminum foil) of the

mats was divided into 4 equally sized rectangles. From each rectangle, 2 strips were cut from each orientation (parallel and perpendicular).

A total of 8 strips were obtained from each mat for each orientation (parallel and perpendicular) to compose the testing sample. Three fiber mats were produced from three different batches of the solutions. This resulted in 24 strips per group and orientation (n = 24). Displacement (mm) was calculated by dividing the time (sec) required to tear the strip by the elongation rate (0.2 mm/s). The strain was obtained by dividing the displacement by the gauge length. The load was registered in gram force. The areal density was calculated from the division of the weigh of the nanofibers(g) strips by its area in m^2.

The specific stress in g/Tex was given by the following Eq. (1):

$$Stress\left(\frac{g}{Tex}\right) = \frac{[Force\,(g) \div sample\,width\,(mm)]}{[Areal\,density\,(g/m^2)} \quad (1)$$

The stress in MPa was calculated from the following Eq. (2):

$$Stress\ (MPa) = 9.8 \times Stress\ (g/Tex) \times density\ of\ material\ (g/cc) \quad (2)$$

Ultimate tensile strength (UTS), elastic modulus (E), yield strength (YS) and elongation at maximum stress (EMS) were calculated from the stress/strain plots (Fig. 1).

2.4.2. *Morphological characterization of nanofiber mats*

The characteristics of PAN nanofibers and PAN with NCC nanofibers were observed first under an optical microscope (Nikon Eclipse LV100 Optical Microscope, Tokyo, Japan). Fibers were collected at the beginning of electrospinning process by manually placing a glass slide in front of the collector plate. After fibers have been visually detected on the surface of the glass, the lamina was taken to the optical microscope and evaluated under 5, 20, and 50× magnifications.

Scanning electron microscope (SEM S-238ON, Hitachi, Tokyo, Japan) was used to evaluate the electrospun mats with an acceleration voltage of 10 kV. Randomly selected areas of each mat were cut in 5 × 5 mm squares and mounted on a stub with carbon tape (n = 3). The stubs were then coated with platinum/palladium (Pt/Pd) with an ion sputter coater (Hitachi E-1030 Ion Sputter Coater, Hitachi, Tokyo, Japan). Random images were taken from the selected pieces of each mat. Average fiber diameter was calculated based on 15 random measurements from pictures taken at the same magnification with an image software (ImageJ, NIH, USA).

Transmission electron microscope (TEM, JEOL, JEM-1400, Tokyo, Japan) was used to morphologically characterize the NCC particles based on similar studies [23]. An aqueous suspension of NCC powder at a concentration of 0.001% in weight was stirred overnight at room temperature. 1 ml of the NCC suspension was mixed for 30 s with 1 ml Uranyl acetate solution (5% w/v) in an Eppendorf vial. A droplet (2 μl) of the mixed suspension was directly applied to a TEM grid with ultra-thin carbon tape. The grids were left to dry in a dust-free environment. The equipment was operated with accelerating voltage of 80 kV, and NCC was identified at 10.000× magnification.

Table 1 – Experimental dental resin and viscosity.

Proportion	Components	Weight %	Viscosity (mPa s)
50:50	BisGMA	49.375	267
	TEGDMA	49.375	
	CQ[a]	0.25	
	EDMAB[a]	1	

Abbreviations: BisGMA: bisphenol A-diglycidyl ether dimethacrylate; TEGDMA: triethylene-glycol dimethacrylate; CQ: camphoroquinone; EDMAB: ethyl N,N-dimethyl-4-aminobenzoate.
[a] Required for photoactivation and polymerization of the resin.

2.5. *Crystallinity of NCC*

The crystallinity of NCC was analyzed by powder X-ray diffraction (Bruker D8-Advance X-ray diffractometer, D8 Advance, Bruker, MA, USA) utilizing NCC powder packed in standard Bruker sample holder and rotated. The generator was set at 40 kV and 40 mA. The machine was operated under Bragg-Brentano configuration, with Copper $K\alpha_1$ and $K\alpha_2$, Nickel filter and a LynxEye silicon strip as detector.

2.6. *Molecular component analysis*

PAN raw polymer (Scientific Polymer Products, Ontario, NY, USA), NCC (Alberta Innovates, Alberta, Canada), nanofiber mats of pure PAN and mats containing NCC were analyzed by a Fourier transform infrared spectrometer (FTIR) equipped with attenuated total reflectance (ATR) (IRPrestige-21 FTIR-8400S, Shimadzu, Kyoto, Japan). The samples were compressed against the ATR crystal and scanned 36 times at a definition of 4 cm^{-1} within the spectra of 400 and 4000 cm^{-1}. The equipment was operated in absorbance mode with Happ-Genzel function.

2.7. *Creation and characterization of nanofiber reinforced dental composites*

2.7.1. *Preparation of BisGMA/TEGDMA monomer blends*

Resin monomers (Table 1) were provided by Esstech (Essington, PA, USA). Bisphenol A-diglycidyl ether dimethacrylate (BisGMA), triethylene-glycol dimethacrylate (TEGDMA), camphorquinone (CQ) and ethyl N,N-dimethyl-4-aminobenzoate were weighed in an analytical balance (Shimadzu, ATX 124, Kyoto, Japan). Monomers were manually mixed with a spatula at room temperature in an Ambar glass vial, protected with aluminum foil. After the initial mix, the vial was left on a stirring plate overnight in a yellow room.

A total of 120 ml of experimental resin was produced. This amount was sufficient to produce all specimens, therefore avoiding variations between batches during the manufacturing process of the composites.

2.7.2. *Production of nanofiber reinforced composite*

Samples of the nanofiber mat were cut from random areas of the mat in the perpendicular orientation (higher mechanical properties as described in chapters 2 and 3) with a

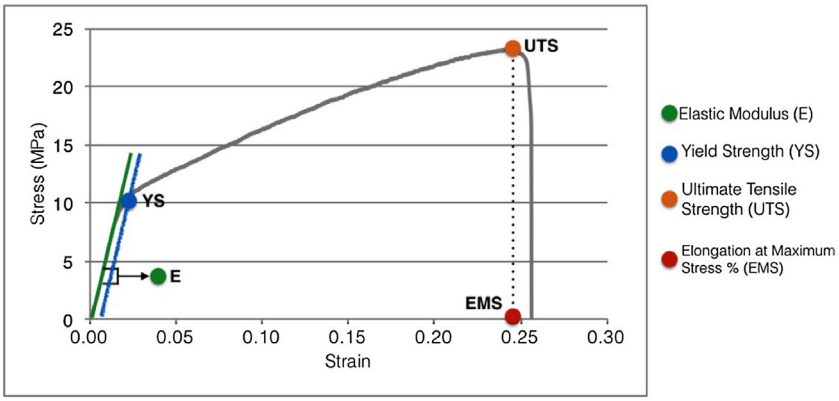

Fig. 1 – Representative stress/strain plot. Elastic Modulus (E) was obtained from the steepest part of the low strain section of the plot by dividing the variation in stress by variation in strain. Yield Strength (YS) was determined by constructing a line parallel to the linear portion of the graph and offset at 0.3% from the origin in the horizontal axis. Ultimate Tensile Strength (UTS) was the set as the highest value on the vertical axis of the graph. Elongation at Maximum Stress (EMS) was obtained in percentage by multiplying by 100 the strain value (horizontal axis) at the point of UTS.

14.5 × 24.5 mm dimension. The cut samples were stacked dry in a mold (2 × 15 × 25 mm) of polyvinyl siloxane (PVS) to determine the maximum number of sheets (nanofiber mats) that would fit in the mold. It was determined that 5 sheets of cut samples would fill the mold. For each available mold, 5 sheets of mat were cut, separated and weighed in an analytical balance to later determine the mass ratio of fiber to resin of the final, cured block of composite. Blocks of pure resin blend were produced as control group (no fiber), and blocks containing PAN nanofibers with and without the addition of 3% NCC were produced as experimental groups.

To produce the composite blocks, the experimental resin blend was first placed in vacuum overnight (−28 mm Hg) to remove air bubbles from the handling and mixing. Following, separate 180 μl aliquots of the resin were dispensed with a pipette on an aluminum foil. Individual mats were placed on each drop of resin to allow wetting and embedding and then taken to vacuum overnight (−28 mm Hg). Subsequently, embedded mats were stacked one by one in the PVS mold. Each layer was meticulously placed and all visible air bubbles were manually removed with the aid of a spatula. Once the mold was filled with the embedded mats, a thin sheet of transparent cellulose acetate was placed on the top and covered with a glass slide. Pressure clamps were placed at each end of the glass slide to hold constant pressure to the block. After that, the samples were light cured (Bluephase 2.0i; Ivoclar Vivadent, Liechstein, Germany) by sequential exposures of 30 s in 9 different spots to cover the entire block surface. The irradiance of the curing light was measured and kept in the range between 1380–1420 mW/cm^2. After curing, the clamped block was left in a dark room overnight. Next day, the block was removed from the mold and the other side was light-activated using the same protocol. Once both sides were cured, the block was removed and hand-polished with a #320 grit sandpaper. The final block was weighed to determine the fiber/resin mass ratio using the respective, previously measured weight of the fiber mats that composed the block. The cured block was kept in water at 37 °C for 24 h until further processing.

2.7.3. *Flexural properties testing*

Testing was performed according to ISO 10477 standard. Beams measuring 25 × 2 × 2 mm were produced by cutting the composites blocks with a precision cutting machine (SYJ-150 Low Speed Diamond Saw, MTI Corporation, USA). Specimens were stored in water at 37 °C for 5 days before testing.

Three-point bend test was performed in a universal testing machine (Shimadzu Corp., Kyoto, Japan) with a 20-mm span and cross-head speed of 1 mm/min. All beams were tested with load applied to the surface that was first exposed to light-curing. Work of fracture (WF), flexural strength (FS) and flexural modulus (FM) were calculated by a software (Trapezium X, Shimadzu Corp., Kyoto, Japan), using the following Eqs. (3)–(5):

$$WF = \frac{A}{bh} \tag{3}$$

$$FS = \frac{3FL}{2bh^2} \tag{4}$$

$$FM = \frac{L^3 m}{4bh^3} \tag{5}$$

Work of fracture was expressed in kJ/m^2, flexural strength was given in MPa and flexural modulus in GPa. “A” stands for the area under the stress-strain curve, “b” is the width of the sample, “h” is the height of the beam (both in mm). “F” is the maximum applied load in Newtons, “L” is the support spam and “m” is the slope of the initial straight portion of the load-deflection curve.

2.7.4. *Fracture analysis*

Failure features were analyzed at the fractured surfaces. Tested beams were analyzed in two different steps. First, all samples were examined under an optical microscope. Second, randomly selected samples were further examined under a scanning electron microscope (SEM S-238ON, Hitachi, Tokyo, Japan) operated at an acceleration voltage of 10 kV.

2.7.5. *Areal density of fibers in flexural beams*

Estimation of fiber density was performed on fractured beams under SEM. Images at the same magnification (1.5 K) were taken from the fractured sites. The images were transferred to Image J Software and a standard area (417 μm^2) was determined on the images. The number of fibers within the determined area was manually counted. The number of fibers was counted from three separate areas of the examined surface and then reported as the average number of fibers per area.

2.8. *Statistical analysis*

Comparison between the mechanical properties of parallel and perpendicular orientation from the nanofibers mats were performed by multiple Student t-test. Two-way ANOVA was used to test if the viscosity of polymeric solutions were different between different batches of PAN 11% with and without 3% NCC. One-way ANOVA was used to evaluate the effect of NCC on the tensile properties. All data analysis was conducted with Sigma Plot software (Systat Software, San Jose, USA) at $\alpha = 5\%$. Groups that failed the normality test had their statistical tests changed accordingly. Mann–Whitney U test was used instead of Student t-test.

To determine the effect of adding fibers with and without NCC to resin blocks, a One-way ANOVA and a Holm-Sidak post hoc test were used. Level of significance was set at $\alpha = 5\%$ and Sigma Plot software was used.

3. Results

3.1. *Viscosity measurements*

The mean viscosity of the three batches of PAN 11% solutions were 436, 440, and 440 mPa s respectively. When NCC was added to the solution, the three batches yield mean viscosity values: 439, 440 and 443 mPa s. There was no statistical difference among the batches of both groups ($p > 0.05$).

3.2. *Nanofiber mats properties*

3.2.1. *Tensile properties of nanofibers mats*

Overall, the addition of NCC particles to the PAN nanofibers increased most mechanical properties. The mats showed anisotropic behaviour, with significantly higher properties at the perpendicular orientation, and significantly superior elongation in the parallel orientation (Table 2). Strips that were mechanically stressed by the handling prior testing were not included in the sample (not tested), resulting in n <24 in some groups.

3.2.2. *Morphological characterization of nanofiber mats and NCC*

Scanning electron microscopy (SEM) images of 0% NCC (Control) group showed fibers with random distribution with uniform diameter (Fig. 2). Group 3% NCC (Fig. 3) also showed randomly distributed fibers with a regular diameter. There was a significant difference in fiber diameter among the groups (Table 3). The presence of NCC increased fiber diameter.

Table 2 – Effects of NGC on tensile properties of nanofiber mats.

	UTS (MPa)			E (GPa)			EMS (%)		
	PAR	PER	t-Value	PAR	PER	t-Value	PAR	PER	t-Value
0% NCC	10.55 (2.75)^{A} (n = 23)	17.65 (4.25)^{A*} (n = 21)	−6.62	0.14 (0.04)^{B} (n = 23)	0.43 (0.06)^{B*} (n = 21)	−18.17	37 (6)^{A*} (n = 23)	19 (7)^{A} (n = 21)	9.27
3% NCC	11.98 (3.08)^{A} (n = 22)	18.63 (5.20)^{A*} (n = 23)	+	0.19 (0.07)^{B} (n = 22)	0.34 (0.06)^{C*} (n = 23)	−7.72	41 (9)^{A*} (n = 22)	20 (7)^{A} (n = 23)	8.87

Different letters (one-way ANOVA) indicate significant difference between the values for each property and orientation ($p < 0.05$); * (t-test) indicate significant difference between PAR and PER for NCC dispersion ($p < 0.05$). Abbreviations: PAR: parallel to rotatory drum axis; PER: perpendicular to rotatory drum axis; UTS: ultimate tensile strength; E: elastic modulus; EMS: elongation at maximum stress. +t-value not available (Mann–Whitney performed).

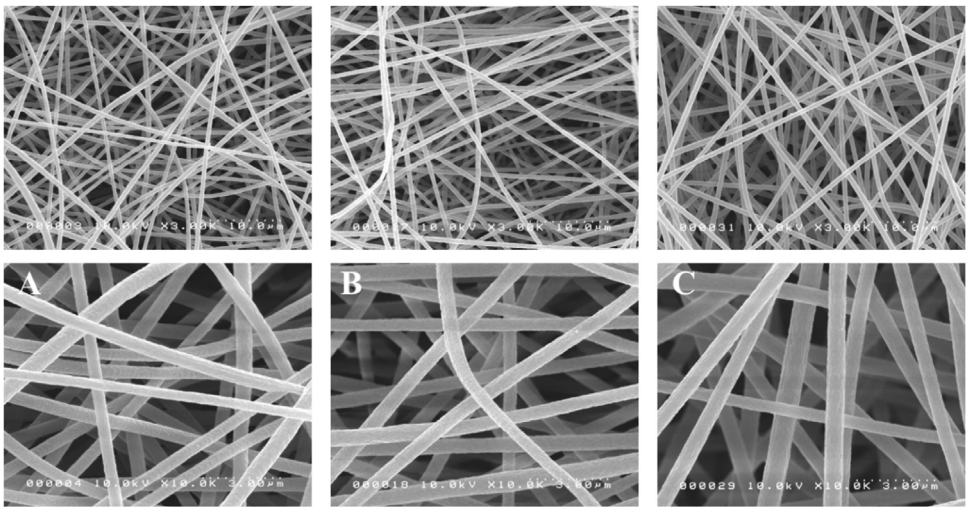

Fig. 2 – SEM of 0% NCC (PAN 11% Control) group.A: Batch 1; B: Batch 2; C: Batch 3.

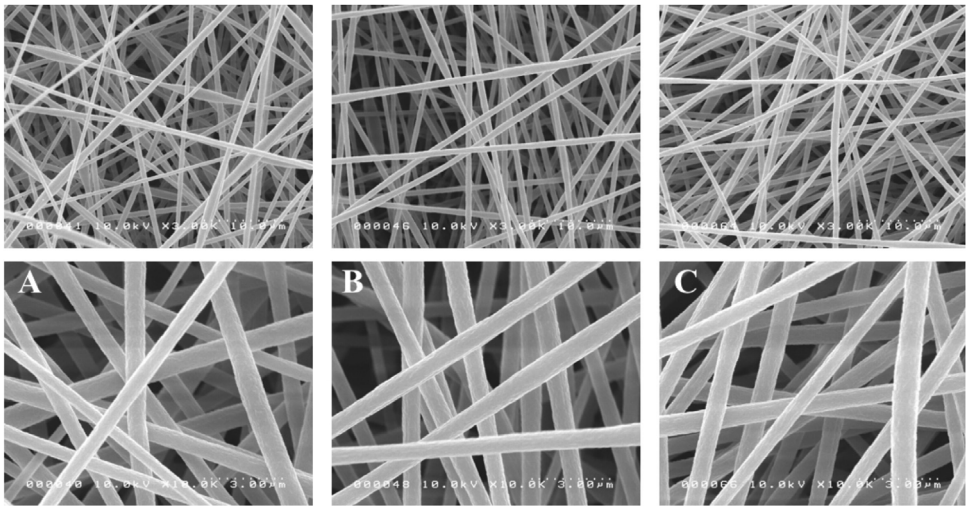

Fig. 3 – SEM of 3% NCC group. A: batch 1; B: batch 2; C: batch 3.

Table 3 – Fiber diameter according to groups.

Group	Average diameter (SD)
0% NCC (PAN 11% control) n = 45	570 (130) nm^{B} range: 358–933 nm
3% NCC n = 45	692 (159) nm^{A} range: 392–693 nm

Different letters (one-way ANOVA) indicate significant difference between the values ($p < 0.05$).

Transmission electron microscopy showed NCC particles (Fig. 4) with an average length of 173 nm (range: 113–246 nm) and average diameter of 12 nm (range: 8–15 nm).

3.3. *Molecular component analysis*

The FTIR (Fig. 5) showed similar spectra for the pure PAN polymer, PAN nanofiber and PAN with NCC at 3%. The FTIR spectrum of pure NCC matched the cellulose spectrum from the database.

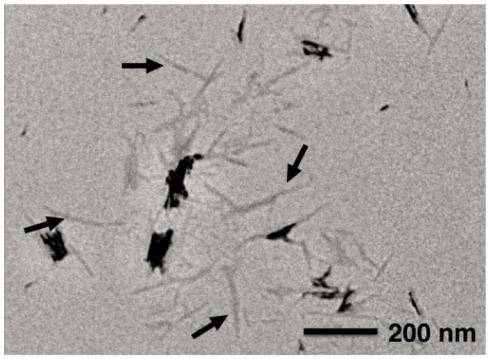

Fig. 4 – TEM of NCC particles. NCC showed a rod-like appearance with a length close to 200 nm and a diameter around 12 nm.

3.4. *X-ray diffraction*

The powder X-ray diffraction interference pattern (Fig. 6) showed peaks on the 20–30 and 30–40 range of the theta scale.

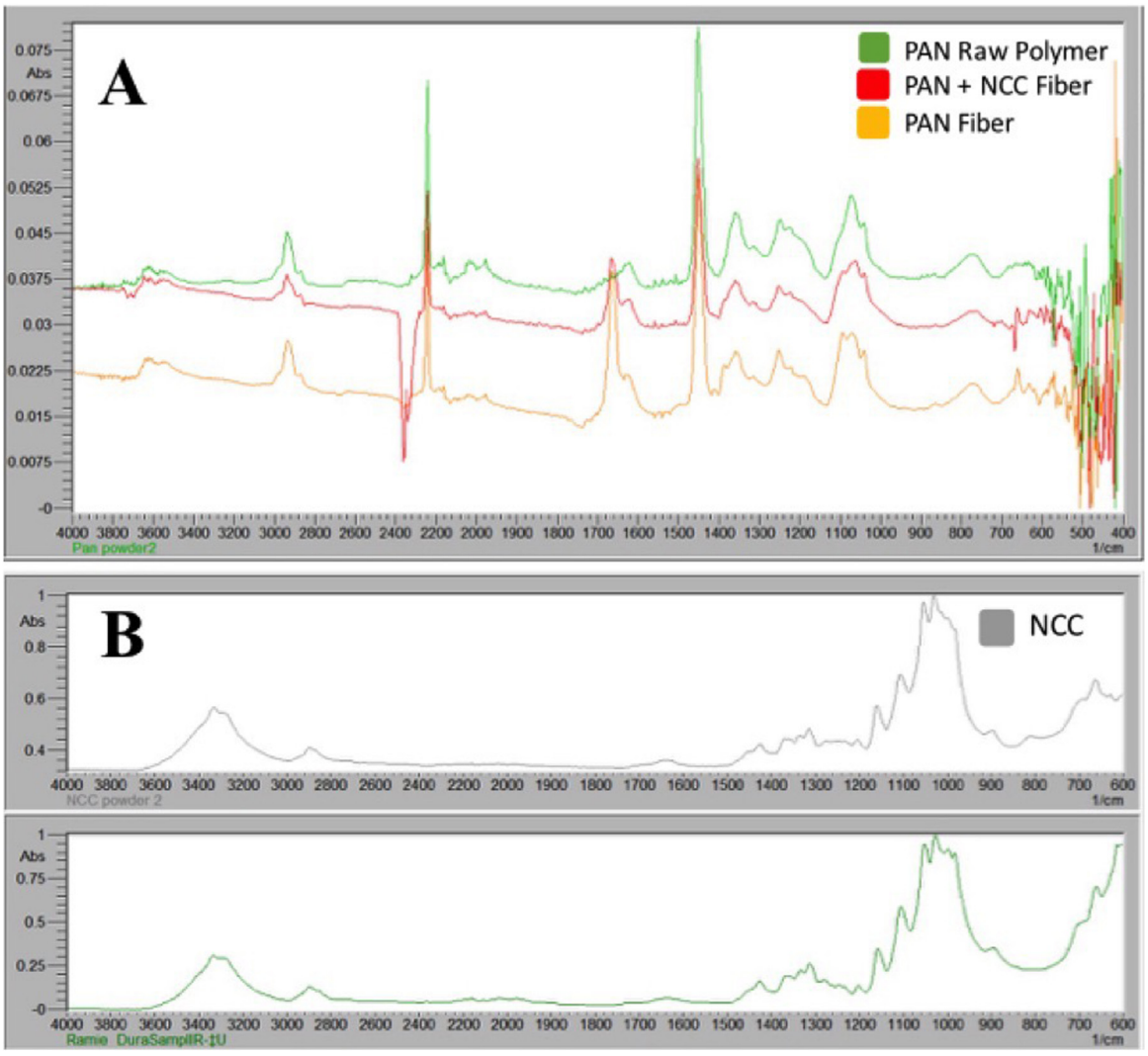

Fig. 5 – FTIR Readings. A: Green reading represents pure PAN polymer spectrum as provided by the manufacturer; Red reading shows a PAN fiber with 3% NCC where differences can be seen. A slight peak can be observed in the 1600–1700 range and a significant peak at the range of 2200–2400; Yellow spectra establishes a similar peak, but with higher intensity, in the 1600–1700 range as the red reading, and do not show a negative peak in the 2400 range. B: Grey reading represents NCC powder, green spectra shows FTIR database for cellulose. (For interpretation of the references to colour in this figure legend, the reader is referred to the web version of this article).

It indicates the crystalline structure of the NCC powder used in this study.

3.5. *Properties of nanofiber reinforced experimental dental composites*

3.5.1. *Flexural strength*

Flexural strength was significantly higher in composites produced with NCC-containing fibers ($p < 0.05$). Flexural modulus was statistically reduced when composites had fibers, regardless of the presence or not of NCC in the fibers ($p < 0.05$). The addition of nanofibers alone, followed by the addition of the nanofibers containing NCC resulted in significant gradual increases in the work of fracture($p < 0.05$). The addition of PAN nanofibers resulted in significantly higher energy necessary to break the specimens; and when fiber-containing NCC were added, further significant increases were observed in the work of fracture (Table 4).

3.5.2. *Fracture analysis*

Analysis of fractured beams under optical microscope showed that samples from control group (no fiber) had characteristic features of a brittle-like material. Mirror, mist, hackles, and compression curl were all detected in the samples examined. Groups containing fibers (with and without NCC) did not exhibit these characteristics under light microscopy, except for compression curl.

Under scanning electron microscopy, a more evident difference between the fracture pattern of non-reinforced and reinforced beams was detected (Fig. 7). The fibers were readily distinguished from the resin matrix, randomly distributed within the resin matrix (Fig. 8A, B). When beads were present,

Table 4 – Effects of the presence of NCC in PAN nanofiber reinforced dental composites.

Groups	Flexural strength MPa (SD)	Flexural modulus GPa (SD)	Work of fracture KJ/m^2 (SD)
Resin blend (no fiber) (n = 18)	94.91 (11.43)^{B}	2.85 (0.21)^{A}	5.46 (1.88)^{C}
0% NCC–PAN (n = 47)	99.03 (8.80)^{AB}	2.62 (0.21)^{B}	7.11 (2.09)^{B}
3% NCC– PAN (n = 42)	101.39 (5.92)^{A}	2.60 (0.17)^{B}	8.05 (1.62)^{A}

Different letters (one-way ANOVA) indicate significant difference between the values for each property ($p < 0.05$).

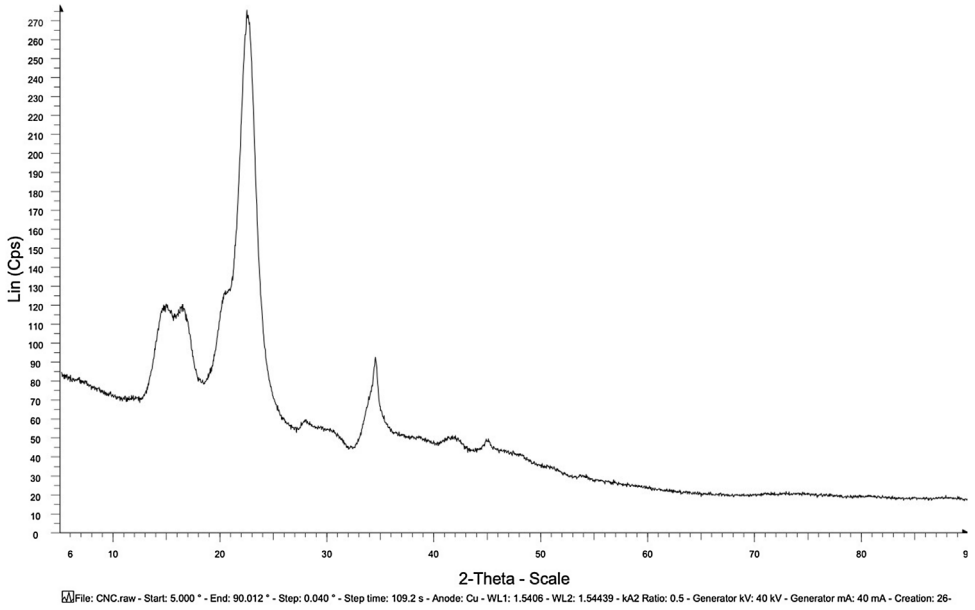

Fig. 6 – X-Ray Diffraction. The diffraction pattern shows a constructive interference which satisfies Bragg's law. Sharp peaks indicate that NCC had its atoms organized to form crystalline structures.

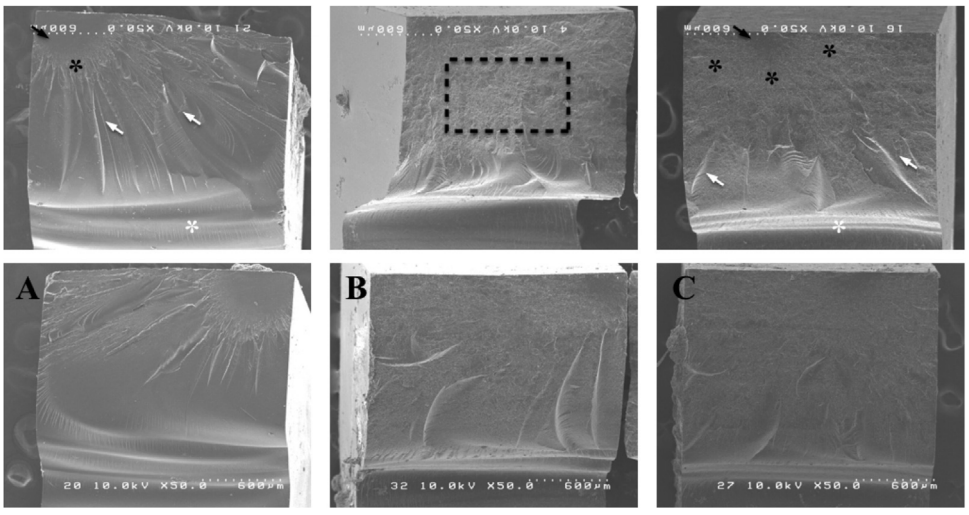

Fig. 7 – SEM images of fractured surfaces of tested beams. All beams have the load side oriented up. A: Control (no fiber) group with typical fractographic characteristics. Mirror (black arrow) followed by mist (black asterisk). Long hackle lines (white arrows) are well connected to the mist and compression curl (white asterisk); B: PAN 11% beams, features are present but less prominent. Dotted square shows a change in the pattern of fracture with a rough aspect. Hackle lines are less in number and shorter. End of mist area is not as evident as in control group. C: PAN 11% + 3% NCC group presented similar appearance as in PAN 11% group. Mirror (black arrow) is smaller, while mist area (black asterisk) is larger. Hackle lines (white arrows) are shorter, shifted towards compression curl (white asterisk) and can not be traced back to the mist area.

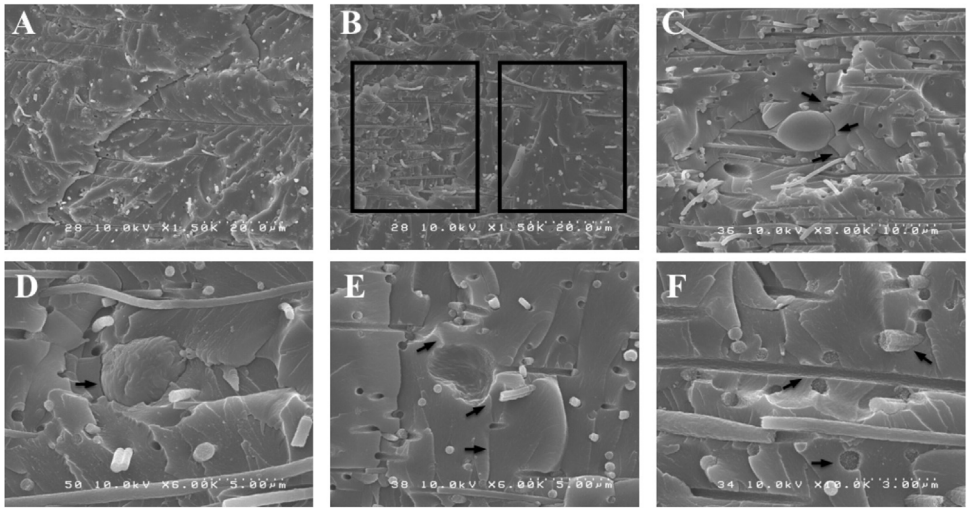

Fig. 8 – Nanofiber dental composite features. A: PAN 11% group presents fibers randomly oriented; B: PAN 11% + NCC 3%, squares show that areas with less fibers (right square) present more evident crack propagation (hackle lines). In areas with denser fiber concentration (left square) this characteristic is not so prominent; C: PAN 11% + NCC 3% the presence of beads appeared to deviate propagation of fracture lines (arrows); D: PAN 11% + NCC 3%, crack propagation across beads seemed to follow the weaker path at the interface between the bead and the matrix, thus deviating the fracture plane; E: PAN 11% + NCC 3% a detached bead leaves behind the perfect copy of its surface on the resin matrix. The fracture plane does not propagate across the bead (arrows); F: PAN 11% + NCC 3%, cross-sections of the fibers show a bundle-type appearance (a nanofiber seems to be composed of several, smaller, fibrils). The surface of the fibers is not smooth, confirmed by the impression left on the matrix (arrows).

they were associated with a perceived deviation of the fracture propagation planes and direction (Fig. 8C–E).

There were virtually no voids detected between the fibers and the matrix in the examined samples (Figs. 8F, 9 D). Generally, fibers were not damaged or altered by the manufacturing process of the composites. Interestingly, individual fibers in both groups (with and without NCC) seemed to be formed by several distinct fibrils bound together to form the reinforcing fiber (Fig. 9A).

The fibers seemed to integrate well with the resin matrix, indicating a good wetting of the fibers by the resin, despite no attempts to functionalize the fibers in this study (Fig. 8F). In some areas, the resin matrix appeared to intimately cover the fiber (Fig. 9B). No complete fiber pull out could be observed, thus corroborating the intimate contact between fibers and matrix (Fig. 9C).

3.5.3. *Areal density of fibers on flexural beams and mass ratio for fiber in composite blocks*

The amount of fibers per mm^2 (Table 5) was very similar for both groups (with and without NCC). Overall, around 120,000 fibers were present per mm^2. The average mass ratio for PAN fibers without NCC was 4.7% and with NCC was 5.8%.

4. Discussion

Based on the results of the present study, the null hypothesis was rejected.

It was found that the stacking of 11% PAN nanofibers alone to built an experimental dental composite increased significantly the work of fracture and resulted in no statistically significant changes in flexural strength. However, when 3% NCC was incorporated in the PAN fibers and then inserted in our resin-based composites, the increases were statistically significant for both work of fracture and flexural strength.

The addition of random nanofiber mats, regardless of the presence of NCC, reduced significantly the flexural modulus. Our findings mostly agree with previous work using analogous methodology [6]. In their work, 7% PAN nanofibers were produced and stacked in different concentrations, using different viscosity resin-blends. It was found that 5.4% weight fraction of PAN nanofibers mat produced the highest and most significant increase of work of fracture. Such finding was corroborated in this study. Differently from Vidotti et al. [6], our study showed a significant decrease in flexural modulus. The increase in flexural properties herein reported was also found in studies [8] that used different polymer. Nylon 6 in similar mass concentrations (5–7.5%) increased flexural properties of 50/50 BisGMA/TEGDMA blends [8].

When compared to studies [15] that also used nanoparticles in their fibers to reinforce dental composites, our findings are partially in agreement. Borges et al found that random fibers with 0.5% of carbon nanotubes significantly increased flexural strength [15]. The presence of carbon nanotubes in random nylon 6 fibers was only effective as a reinforcing agent at 0.5%. When 1.5% was used, there was no difference from control group [15]. However, when NaF crystals were used, no significant role on flexural properties of BisGMA/TEGDMA blends was observed [14].

In the present experiment, a fixed concentration of NCC was used. NCC is known to reinforce nanofibers by a percolation network formed between the hydroxyl groups available on its surface and the radicals from the polymeric matrix [24]. This close interaction can explain why NCC-containing PAN

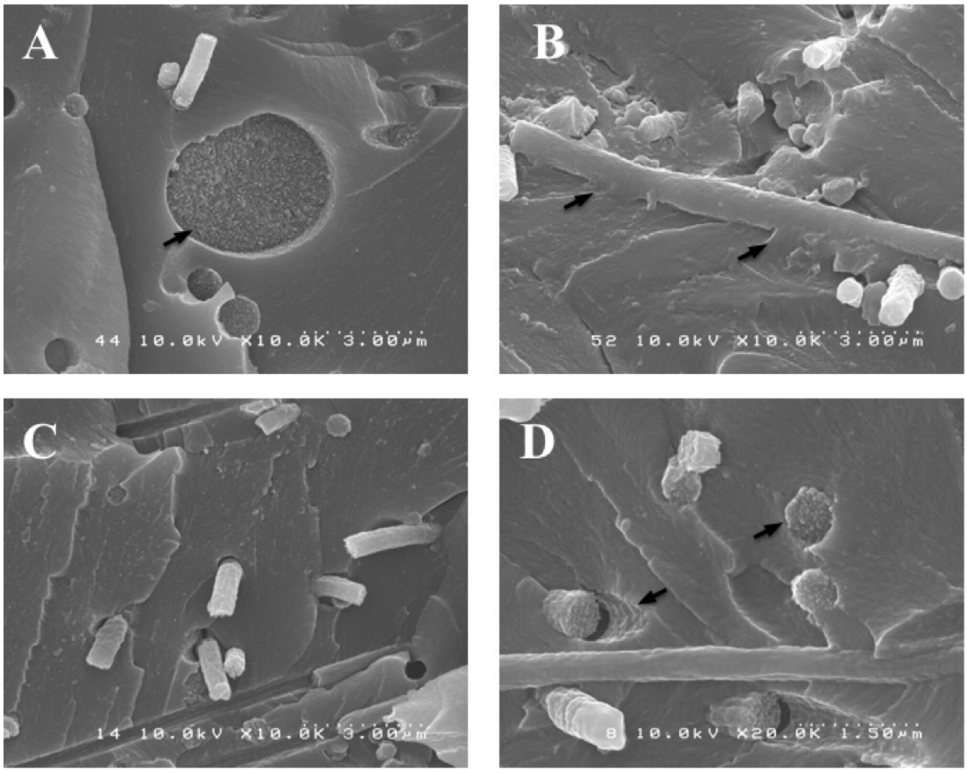

Fig. 9 – Findings on nanofiber reinforced composites. A: Sectioned bead, showing the bundle-type appearance commonly found in cross-sections of the fibers. Nanofibers seems to be formed from multiple fibrils; B: Arrows point the resin flowing over a fiber, with intimate contact; C: Complete pull out of the fiber was not observed in most of the fibers. Fibers fractured cohesively either slightly above or below the fracture plane; D: Sectioned nanofibers from PAN 11% groups features the appearance of bundle-type (right arrow) and also the surface is rough and leaves an impression on the matrix (left arrow).

Table 5 – Measurements of areal density of fiber on flexural beams.

0% NCC (PAN 11%)			PAN 11% + 3% NCC		
Batch #1	Batch #2	Batch #3	Batch #1	Batch #2	Batch #3
32	40	62	37	59	64
45	51	61	38	58	58
50	48	64	31	60	49
Average: 42.3	Average: 46.3	Average: 62.3	Average: 35.3	Average: 59	Average: 57
Average: 50.3 per 417 μm^2			Average: 50.4 per 417 μm^2		
Average: 119,904/mm^2			Average: 120,863/mm^2		

nanofibers resulted in the highest and statistically superior flexural strength and work of fracture.

To our knowledge, this is the third report using composite nanofibers to mechanically improve dental resins, and the first using NCC. In fact, the combination of nanofibers with nanoparticles is a complex matter. Interactions between particles, polymers, solvents and parameters involved in electrospinning can directly affect the dispersion of the fillers in the nanofiber, and by consequence completely change its characteristics [11,25,26].

In the past, nanoparticles were used to produce commercially available dental composites. Their primary issue was regarding the distribution of the particles within the matrix. The high surface energy caused particles to agglomerate and lose the advantage of the nano scale [27]. Findings in our study can serve as a fundamental study to proof the principle of using nanoparticles distributed by nanofibers to reinforce dental composites. Such combination could bring together the positive reinforcement of the nano-particles (dispersed in the fibrous matrix) with the advantageous reinforcement by fibers.

Also, alignment and post-spinning treatments are associated with better mechanical results [7,15]. It is important to stress that in this study fibers were used and tested as-spun.

The increased mechanical properties using PAN and NCC-containing PAN are converse to some literature. Inferior performance of only PAN fibers had been attributed to poor interfacial bonding between fiber and matrix [10]. Such discrepancy can be further explained by our SEM findings.

Scanning electron microscopy images of fibers embedded in dental resin showed a good wetting by the matrix

and no pull-outs were observed on the fractured surface, even though no attempts were made to functionalize PAN and NCC-containing PAN nanofibers. The viscosity (50/50 BisGMA/TEGDMA) of the monomer blend used might have facilitated infiltration and wetting process. Poor wetting was considered crucial to explain the fact that incorporation of cellulose acetate significantly reduced mechanical properties of dental and epoxy resins [9].

Additionally, care was taken to properly characterize fiber density in flexural beams (Table 3). Since the fiber density was not different among groups, we credited the differences in properties to the potential reinforcing effect of NCC. Additionally, the mass fraction (PAN 11% 4.7% and PAN 11% + 3% NCC 5.8%) can be associated with heavier fibers when NCC was added and not due to a higher number of fibers.

Another aspect that conflicts nanofiber technology with the data here presented is the presence of beads. The presence of beads in the fibers has long been regarded as not desirable in nanofiber production, although no clear explanation is found to justify the apparent negative effect of the presence of beads [28,29]. Beads were found in our study and, contrary to odds, they seemed to provide a positive effect in deflecting the crack propagation and, along with the fibers themselves, resulted in improved work of fracture of the composites.

5. Conclusions

The presence of NCC in the PAN nanofibers resulted in significant improvement of work of fracture and flexural strength of experimental composite beams. This fundamental study warrants future investigation in the use of electrospun nanofibers with nanoparticles. NCC was found to be a suitable nanoparticle to reinforce experimental dental composites by incorporation via nanofiber.

Acknowledgements

Partially supported by UBC Start-Up funds to APM and RMC, and funds from CNPq/CAPES, Brazil.

REFERENCES

[1] Opdam NJM, van de Sande FH, Bronkhorst E, Cenci MS, Bottenberg P, Pallesen U, et al. Longevity of posterior composite restorations: a systematic review and meta-analysis. J Dent Res 2014;93:943–9, http://dx.doi.org/10.1177/0022034514544217.

[2] Ferracane JL. Resin-based composite performance: are there some things we can't predict? Dent Mater 2013;29:51–8, http://dx.doi.org/10.1016/j.dental.2012.06.013.

[3] Ferracane JL. Resin composite—state of the art. Dent Mater 2011;27:29–38, http://dx.doi.org/10.1016/j.dental.2010.10.020.

[4] Hamilton MF, Otte AD, Gregory RL, Pinal R, Ferreira-Zandoná A, Bottino MC. Physicomechanical and antibacterial properties of experimental resin-based dental sealants modified with nylon-6 and chitosan nanofibers. J Biomed Mater Res B Appl Biomater 2015;103:1560–8, http://dx.doi.org/10.1002/jbm.b.33342.

[5] Tian M, Gao Y, Liu Y, Liao Y, Xu R, Hedin NE, et al. Bis-GMA/TEGDMA dental composites reinforced with electrospun nylon 6 nanocomposite nanofibers containing highly aligned fibrillar silicate single crystals. Polymer 2007;48:2720–8, http://dx.doi.org/10.1016/j.polymer.2007.03.032.

[6] Vidotti HA, Manso AP, Leung V, do Valle AL, Ko F, Carvalho RM. Flexural properties of experimental nanofiber reinforced composite are affected by resin composition and nanofiber/resin ratio. Dent Mater 2015;31:1132–41, http://dx.doi.org/10.1016/j.dental.2015.06.018.

[7] Sun W, Cai Q, Li P, Deng X, Wei Y, Xu M, et al. Post-draw PAN–PMMA nanofiber reinforced and toughened Bis-GMA dental restorative composite. Dent Mater 2010;26:873–80, http://dx.doi.org/10.1016/j.dental.2010.03.022.

[8] Fong H. Electrospun nylon 6 nanofiber reinforced BIS-GMA/TEGDMA dental restorative composite resins. Polymer 2004;45:2427–32, http://dx.doi.org/10.1016/j.polymer.2004.01.067.

[9] Boyd SA, Su B, Sandy JR, Ireland AJ. Cellulose nanofibre mesh for use in dental materials. Coatings 2012;2:120–37, http://dx.doi.org/10.3390/coatings2030120.

[10] Lin S, Cai Q, Ji J, Sui G, Yu Y, Yang X, et al. Electrospun nanofiber reinforced and toughened composites through in situ nano-interface formation. Compos Sci Technol 2008;68:3322–9, http://dx.doi.org/10.1016/j.compscitech.2008.08.033.

[11] Ko FK, Li Y, Lin L, Yang H. Multifunctional composite nanofibers. J Fiber Bioeng Inf 2013;6:129–38, http://dx.doi.org/10.3993/jfbi06201302.

[12] Ko F, Gogotsi Y, Ali A, Naguib N, Ye H, Yang GL, et al. Electrospinning of continuous carbon nanotube-filled nanofiber yarns. Adv Mater 2003;15:1161–5, http://dx.doi.org/10.1002/adma.200304955.

[13] Ayutsede J, Gandhi M, Sukigara S, Ye H, Hsu C, Gogotsi Y, et al. Carbon nanotube reinforced *Bombyx mori* silk nanofibers by the electrospinning process. Biomacromolecules 2006;7:208–14, http://dx.doi.org/10.1021/bm0505888.

[14] Cheng L, Zhou X, Zhong H, Deng X, Cai Q, Yang X. NaF-loaded core–shell PAN–PMMA nanofibers as reinforcements for Bis-GMA/TEGDMA restorative resins. Mater Sci Eng C 2014;34:262–9, http://dx.doi.org/10.1016/j.msec.2013.09.020.

[15] Borges ALS, Münchow EA, de Oliveira Souza AC, Yoshida T, Vallittu PK, Bottino MC. Effect of random/aligned nylon-6/MWCNT fibers on dental resin composite reinforcement. J Mech Behav Biomed Mater 2015;48:134–44, http://dx.doi.org/10.1016/j.jmbbm.2015.03.019.

[16] Moon RJ, Martini A, Nairn J, Simonsen J, Youngblood J. Cellulose nanomaterials review: structure, properties and nanocomposites. Chem Soc Rev 2011;40:3941, http://dx.doi.org/10.1039/c0cs00108b.

[17] Cao X, Huang M, Ding B, Yu J, Sun G. Robust polyacrylonitrile nanofibrous membrane reinforced with jute cellulose nanowhiskers for water purification. Desalination 2013;316:120–6, http://dx.doi.org/10.1016/j.desal.2013.01.031.

[18] Lalia BS, Guillen E, Arafat HA, Hashaikeh R. Nanocrystalline cellulose reinforced PVDF-HFP membranes for membrane distillation application. Desalination 2014;332:134–41, http://dx.doi.org/10.1016/j.desal.2013.10.030.

[19] Silva RM, Pereira FV, Mota FAP, Watanabe E, SMCS Soares, Santos MH. Dental glass ionomer cement reinforced by cellulose microfibers and cellulose nanocrystals. Mater Sci Eng C 2016;58:389–95, http://dx.doi.org/10.1016/j.msec.2015.08.041.

[20] Papkov D, Zou Y, Andalib MN, Goponenko A, Cheng SZD, Dzenis YA. Simultaneously strong and tough ultrafine continuous nanofibers. ACS Nano 2013;7:3324–31, http://dx.doi.org/10.1021/nn400028p.

[21] Nataraj SK, Yang KS, Aminabhavi TM. Polyacrylonitrile-based nanofibers—a state-of-the-art review. Prog Polym Sci 2012;37:487–513, http://dx.doi.org/10.1016/j.progpolymsci.2011.07.001.
[22] Peres BU, Vidotti HA, Manso AP, Ko F, Carvalho RM. Nanocrystal cellulose (NCC) as reinforcing agent for electrospun nanofibers. Dent Mater 2015;31:e65–6, http://dx.doi.org/10.1016/j.dental.2015.08.143.
[23] Dong H, Strawhecker KE, Snyder JF, Orlicki JA, Reiner RS, Rudie AW. Cellulose nanocrystals as a reinforcing material for electrospun poly(methyl methacrylate) fibers: formation, properties and nanomechanical characterization. Carbohydr Polym 2012;87:2488–95, http://dx.doi.org/10.1016/j.carbpol.2011.11.015.
[24] Favier V, Chanzy H, Cavaille JY. Polymer nanocomposites reinforced by cellulose whiskers. Macromolecules 1995;28:6365–7.
[25] Li Y, Ko FK, Hamad WY. Effects of emulsion droplet size on the structure of electrospun ultrafine biocomposite fibers with cellulose nanocrystals. Biomacromolecules 2013;14:3801–7, http://dx.doi.org/10.1021/bm400540v.
[26] Beck S, Bouchard J, Berry R. Dispersibility in water of dried nanocrystalline cellulose. Biomacromolecules 2012;13:1486–94, http://dx.doi.org/10.1021/bm300191k.
[27] Jandt KD, Sigusch BW. Future perspectives of resin-based dental materials. Dent Mater 2009;25:1001–6, http://dx.doi.org/10.1016/j.dental.2009.02.009.
[28] Huang Z-M, Zhang Y-Z, Kotaki M, Ramakrishna S. A review on polymer nanofibers by electrospinning and their applications in nanocomposites. Compos Sci Technol 2003;63:2223–53, http://dx.doi.org/10.1016/S0266-3538(03)00178-7.
[29] Fong H, Chun I, Reneker DH. Beaded nanofibers formed during electrospinning. Polymer 1999;40:4585–92.